Nakajima, K., Powers, J. C., Ashe, B. M., & Zimmerman, M. (1979) *J. Biol. Chem. 254*, 4027–4032.
Powers, J. C. (1983) *Am. Rev. Respir. Dis. 127*, S54–S58.
Powers, J. C. Gupton, B. F., Harley, A. D., Nishino, N., & Whitley, R. J. (1977) *Biochim. Biophys. Acta 485*, 156–166.
Renaud, A., Lestienne, P., Hughes, D. L., Bieth, J. G., & Dimicoli, J. L. (1983) *J. Biol. Chem. 258*, 8312–8316.
Sage, H., Woodbury, R. G., & Borstein, P. (1979) *J. Biol. Chem. 254*, 9893–9900.
Schechter, I., & Berger, A. (1967) *Biochem. Biophys. Res. Commun. 27*, 157–162.
Tanaka, T., McRae, B. J., Cho, K., Cook, R., Fraki, J. E., Johnson, D. A., & Powers, J. C. (1983) *J. Biol. Chem. 258*, 13552–13557.
Travis, J., Bowen, J., & Baugh, R. (1978) *Biochemistry 17*, 5651–5656.
Woodbury, R. G., & Neurath, H. (1980) *FEBS Lett. 114*, 189–196.
Woodbury, R. G., Everitt, M. T., & Neurath, H. (1981) *Methods Enzymol. 80*, 588–609.
Yoshida, N., Everitt, M. T., Neurath, H., Woodbury, R. G., & Powers, J. C. (1980) *Biochemistry 19*, 5799–5804.
Zimmerman, M., & Ashe, B. M. (1977) *Biochim. Biophys. Acta 480*, 241–245.

Tryptophan Emission from Myosin Subfragment 1: Acrylamide and Nucleotide Effect Monitored by Decay-Associated Spectra†

Peter M. Torgerson

ABSTRACT: The intrinsic emission due to the tryptophan residues of the heavy chain of myosin subfragment 1 can be divided into three classes, on the basis of spectra associated with lifetimes of 0.72, 4.5, and 8.8 ns. The percentage contribution of each component to the total emission is 9%, 45%, and 46%, respectively. Low concentrations of acrylamide quench the long component with a quenching constant of 14.9 ± 2.9 M^{-1}, while the intermediate and short components are unaffected. Upon addition of ATP the total intensity increases by 17%. The bulk of this increase is in the intermediate lifetime component. Quenching by acrylamide in the presence of ATP again quenches only the long lifetime component, indicating that the tryptophan residues affected by ATP binding are not accessible to the solvent.

The absorption and emission behavior of the tryptophan residues of myosin subfragment 1 (S1)[1] has been utilized in several ways to investigate the structure of S1 and its role in contraction. The degree of polarization of the intrinsic fluorescence was employed in several studies (Dos Remedios et al., 1972; Kishi & Noda, 1983). The effect of nucleotide binding was first examined by Morita (1967), who observed the difference absorption spectrum. Werber et al. (1972) examined the structural features of the nucleotide required for maximal fluorescence enhancement. They also concluded that ATP binding protects two (out of the approximately 20) tryptophan residues of heavy meromyosin from quenching by iodide. Onishi et al. (1973) examined the binding of the fluorescent ATP analogue 1,N^6-ethenoadenosine triphosphate to heavy meromyosin. On the basis of iodide quenching experiments they were able to divide the tryptophan emission into two classes, accessible and inaccessible, and showed that energy transfer to the ATP analogue occurs from the accessible residues.

Advantage has been taken of this nucleotide-induced fluorescence enhancement in the investigation of the kinetics of myosin and actomyosin ATPase activity (Bagshaw & Trentham, 1974; Trybus & Taylor, 1982; Stein et al., 1979; Chock & Eisenberg, 1979). In particular, the fluorescence increase induced by nucleotide has been shown to correspond to more than one step in the hydrolysis cycle (Chock et al., 1979; Johnson & Taylor, 1978). A rapid initial enhancement is produced by ATP binding, followed by a further increase upon hydrolysis. It would be useful if these effects could be linked to alterations in the environment of specific S1 tryptophans.

Recent advances in instrumentation and data analysis have resulted in more thorough analyses of the intrinsic emission characteristics of several proteins (Ross et al., 1981a,b; Privat et al., 1980; Torikata et al., 1979). In particular, more detailed information on the behavior of the emission spectrum during the fluorescence lifetime is not obtainable. Such information includes time-resolved emission spectra, which are the spectra obtained at given times after excitation, and decay-associated spectra, which are those associated with individual components in a multicomponent fluorescence decay. This enables the resolution of the emission into the contributions due to individual tryptophans or groups of tryptophans. An elegant example of such a resolution was obtained with horse liver alcohol dehydrogenase, which contains two tryptophans (Ross et al., 1981b; Knutson et al., 1982). To date, most investigations have employed proteins with small numbers of tryptophan residues and with known sequences and X-ray crystallographic structures. The aim of the present paper is to extend this approach to S1. This is a less tractable problem since S1 contains several tryptophan residues in its heavy chain, about which there is relatively little auxiliary structural information. There is some evidence for segregation of their

† From the Cardiovascular Research Institute, University of California, San Francisco, California 94143. *Received October 4, 1983.* This work was supported by Grants HL-16683, PCM-7922174, and CI-8. This research was carried out during the tenure of a Postdoctoral Fellowship from the Muscular Dystrophy Association.

[1] Abbreviations: S1, chymotryptic subfragment 1 of myosin; TMAC, tetramethylammonium chloride; EGTA, ethylene glycol bis(β-aminoethyl ether)-*N,N,N′,N′*-tetraacetic acid; TES, 2-[[tris(hydroxymethyl)-methyl]amino]ethanesulfonic acid; DAS, decay-associated spectra; ATPase, adenosinetriphosphatase; EDTA, ethylenediaminetetraacetic acid; DTT, dithiothreitol.

0006-2960/84/0423-3002$01.50/0

location in the primary sequence, since limited tryptic digestion of S1 produces three well-defined fragments in which only the heavier two contain tryptophan (Hozumi, 1981). Recent information has determined that the number of tryptophans in the S1 heavy chain is five and has located them in the sequence (M. Elzinga, private communication). I report the resolution of the intrinsic emission of S1 into classes on the basis of decay-associated spectra and the varying response of these classes to acrylamide quenching and ATP binding.

Materials and Methods

Proteins. Myosin was prepared from the back muscles of rabbits (Tonomura et al., 1966). S1 was prepared from myosin by chymotryptic digestion (Weeds & Taylor, 1975). Protein purity and quality were monitored by sodium dodecyl sulfate–polyacrylamide gel electrophoresis, potassium/EDTA- and calcium-activated ATPase activities, and OD_{280}/OD_{260} ratios.

Reagents. ATP (sodium salt) was a product of Sigma. The buffer used in all fluorescence measurements was 80 ± 2 mM tetramethylammonium chloride (TMAC), 1 mM ethylene glycol bis(β-aminoethyl ether)-*N,N,N',N'*-tetraacetic acid (EGTA), 0.5 mM dithiothreitol, and 20 mM 2-[[tris(hydroxymethyl)methyl]amino]ethanesulfonic acid (TES), pH 7.0. TMAC was prepared by neutralizing tetramethylammonium hydroxide (J. T. Baker Chemical Co.) with hydrochloric acid and yielded a buffer with an acceptably small fluorescence background.

Spectroscopic Measurements. Steady-state emission spectra were recorded on an Hitachi Perkin-Elmer MPF-4 spectrofluorometer in the ratio mode. Fluorescence decay data were collected with a single-photon counting instrument consisting of a gated nanosecond flashlamp, sample cavity, optical train, and cooled photomultiplier tube supplied by PRA, Inc. Data collection electronics were essentially as described by Mendelson et al (1975). Due to the nature of the single-photon pulse from the PRA-supplied photomultiplier tube, on-line pulse pileup rejection was not feasible. The electronic modules used to effect this rejection were therefore removed. Photon counting rates were $^1/_{60}$th of the lamp flash rate or less. Data collection was controlled by a Digital Equipment Corp. PDP8/e computer. Data were transferred to a Data General Eclipse 230S computer for analysis.

Quenching Experiments. All experiments were at 4 °C. For each data point, the S1 was prepared at 8×10^{-6} M and brought to the desired acrylamide concentration by addition of a concentrated stock solution, followed by measurement of the steady-state intensity and then the decay curve. For some data points duplicate samples were prepared and their intensity was monitored during the time required for collection of the fluorescence decay. Samples which did not contain ATP were made 5 mM in magnesium chloride, while those which did were made 10 mM in magnesium and 8 mM in ATP by addition of a MgATP stock solution prior to addition of acrylamide. All solutions were adjusted to pH 7.0 before mixing.

Excitation was at 295 nm. Emission wavelengths were selected with interference filters, with a full width at half-maximum of 10 ± 2 nm. Each decay curve typically contained 8×10^5 to 1.2×10^6 total counts, corresponding to 20 000–30 000 counts in the highest channel, and required 1–2 h of data collection. Samples containing ATP showed no intensity change over a 1-h period at these temperature and buffer conditions. If longer collection times were required, duplicate samples were prepared and counted for approximately 1 h each. The concentrations of acrylamide used in this study have been shown to have no effect on the activity of S1 (Ando et al., 1982) and confirmed by the potassium/EDTA ATPase activities to be identical before and after data collection. Due to the low concentrations of acrylamide used, no corrections for its absorbance at 295 nm were necessary.

Data Analysis. The function describing the response to δ-function excitation is assumed to be a sum of exponentials:

$$I(t) = \sum_i \alpha_i \exp(-t/\tau_i) \quad (1)$$

where τ_i is the ith decay constant and α_i is its associated relative intensity. Deconvolution from the actual finite-width lamp pulse was performed by an iterative reconvolution nonlinear least-squares method (Grinvald & Steinberg, 1974; Badea & Brand, 1979). Goodness of fit was evaluated from the reduced χ^2 and the residual autocorrelation curve.

The contribution of the ith component to the intensity observed under constant illumination is given by integrating the decay over all time after the pulse:

$$\int_0^\infty \alpha_i \exp(-t/\tau_i)\, dt = \alpha_i \tau_i \quad (2)$$

Therefore, the fractional contribution of each component is $\alpha_i\tau_i/(\sum_i \alpha_i\tau_i)$. The mean lifetime is then defined as (Inokuti & Hirayama, 1965; Ross et al., 1981)

$$\langle \tau \rangle = \sum_i \alpha_i \tau_i^2 / (\sum_i \alpha_i \tau_i) \quad (3)$$

Decay-associated spectra (DAS) are the fluorescence spectra associated with each decay component individually, i.e., the spectra that would be obtained if emission from all other lifetime components could be suppressed. These are distinct from time-resolved emission spectra, which are the total emission obtained at discrete time intervals after pulsed excitation. There are two methods for calculating DAS. One method resolves n spectra by generating n time-resolved emission spectra and one decay curve capable of determining the n lifetimes (Knutson et al., 1982). This method has the advantage of being relatively rapid and is easily automated. A second method, used here, requires measurement of the steady-state spectrum, a decay curve at each wavelength in the spectrum, and resolution of the individual lifetimes. The decay-associated spectra are then calculated from

$$F_i(\lambda) = F_{ss}(\lambda)[\alpha_i(\lambda)\tau_i / (\sum_i \alpha_i(\lambda)\tau_i)] \quad (4)$$

where $F_{ss}(\lambda)$ is the total steady-state spectrum, $F_i(\lambda)$ is the spectrum associated with the ith component, and the $\alpha_i(\lambda)$'s are the preexponential terms at wavelength λ (Donzel et al., 1974; Ross et al., 1981).

The calculation of DAS assumes that each resolvable lifetime component has a well-defined spectrum associated with it, an assumption that may not always be correct in a multi-tryptophan protein such as S1. Accurate construction of the DAS requires well-determined τ_i values. If the individual τ_i's become too similar, a single decay curve will not yield accurate or reproducible lifetimes. The implicit assumption in the calculation of DAS, however, is that the individual lifetime components are the same at different wavelengths but that their amplitudes vary. As suggested by Knutson et al. (1983) and by Beechem et al. (1983) advantage can be taken of this situation by analyzing all decay curves simultaneously, with the constraint that the lifetimes are the same in all curves but the preexponential terms vary depending on their relative contribution at each wavelength. Since the accuracy of determining a given lifetime varies from one curve to the next depending on its prominence in that particular data set, this

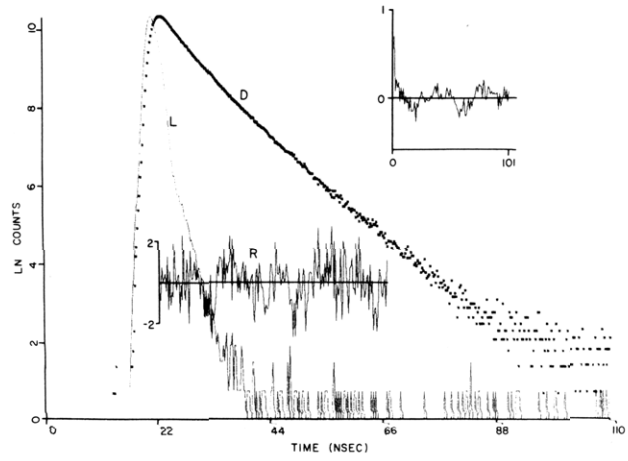

FIGURE 1: Fluorescence decay of 8×10^{-6} M S1 in 80 mM TMAC, 20 mM TES, 5 mM magnesium chloride, 1 mM EGTA, and 0.5 mM DTT, pH 7.0, 4 °C. The lamp curve (L) and data (D) are shown in a semilogarithmic representation. Analysis is from the data maximum to 0.3% of the data maximum, 201 channels at 0.22 ns/channel in this case. The weighted residuals (R) and autocorrelation of the weighted residuals (upper right inset) are shown on a linear scale. The autocorrelation is calculated channel by channel and is displayed over half the range used for the data analysis. Excitation is at 295 nm, and emission is at 350 nm. Fitting parameters are $\alpha_1 = 0.374$, $\tau_1 = 0.63$, $\alpha_2 = 0.366$, $\tau_2 = 4.23$, $\alpha_3 = 0.230$, $\tau_3 = 8.65$, and $\chi^2 = 1.156$.

method allows accurate determination of lifetimes that are much closer together than those which could be reliably extracted from a single decay curve. This procedure, in conjunction with the steady-state spectrum, provides all the information necessary to compute the DAS from eq 4.

The necessary calculations can be performed by using a simple modification of our nonlinear least-squares analysis software. The individual lifetimes are sought by using a grid search algorithm (Bevington, 1969). At each step in the grid, the best fit for the α_i's in each data set is evaluated by the usual Marquardt algorithm, and overall goodness of fit is evaluated from the sum of the individual χ^2 values. Iteration continues until this sum is minimized to a specified degree.

Results

A representative curve of the experimental lamp and the emission intensity of the tryptophans of S1 vs. time is shown in Figure 1. The lamp and data are plotted in a semilogarithmic representation, while the weighted residuals and their autocorrelation function are shown in a linear scale. A random distribution of these last two curves about zero is indicative of a satisfactory fit. The autocorrelation function emphasizes any systematic errors such as radio-frequency interference that may be obscured by noise in the residuals themselves (Grinvald & Steinberg, 1974). Attempting to fit to two decay terms yields a χ^2 of 2.3 and a systematic deviation in the autocorrelation of the weighted residuals, indicating an unsatisfactory fit. A three-component analysis yields a reduced χ^2 of 1.16. As shown in Figure 1, the fit now superimposes with the experimental points and the residuals and their autocorrelation appear to be distributed randomly with time, indicating a satisfactory fit to the data. A requirement for concluding that each of these three lifetimes characterizes a class of tryptophans, each with its own spectral distribution, is that analysis of decay curves at different wavelengths yield identical lifetimes but different preexponential weights. This is so for S1 under the conditions given in Figure 1. Analysis of decay curves from 320 to 380 nm yields lifetimes of 0.82 ± 0.14, 4.68 ± 0.18, and 8.71 ± 0.21 ns. All errors are expressed as

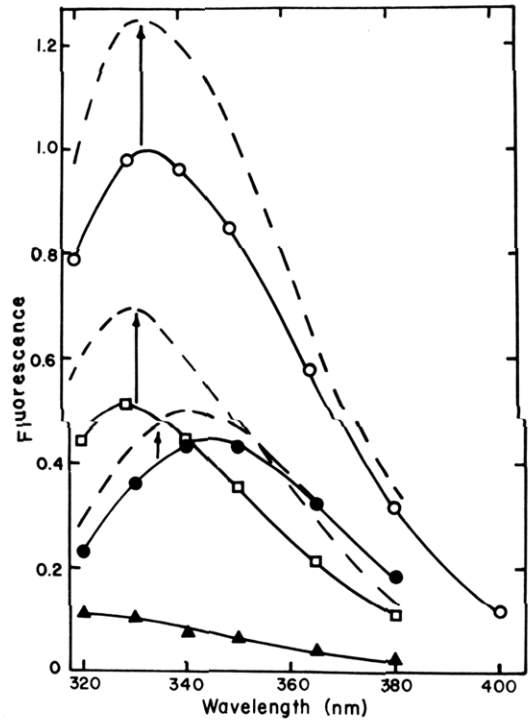

FIGURE 2: Steady-state and decay-associated emission spectra for S1. Conditions are in Figure 1. (○) Total intensity; (●) long lifetime component; (□) intermediate lifetime component; (▲) short lifetime component. Dashed lines indicate the DAS of the corresponding curves in the presence of MgATP.

standard deviations. These results are obtained by analyzing each curve individually with all parameters free and then averaging the lifetimes obtained at all wavelengths. Simultaneous analysis of all curves yields identical values within error. The decay-associated spectra can be constructed as given by eq 4 (Figure 2). The long lifetime component has a spectrum which peaks at about 345 nm, that of the intermediate lifetime has a maximum at about 330 nm, and the spectrum of the short lifetime component appears to level off at about 320 nm (although the lack of data below 320 nm prevents accurate location of its maximum).

When the intrinsic fluorescence is quenched by the addition of acrylamide, the individual lifetimes become more similar. Analysis of a decay curve at a single wavelength is no longer able to resolve reliably the individual decay parameters. Simultaneous analysis of data sets at all wavelengths is then necessary and yields reproducible lifetime and intensity values. The DAS for S1 under the same conditions of solvent and temperature, but in the presence of 40 mM acrylamide, are shown in Figure 3. The spectra of the short and intermediate lifetime components appear unaffected by the quencher, both in intensity and in location, and their decay constants are unchanged within experimental error. The lifetime of the long component, however, is decreased to 7.26 ns by this concentration of acrylamide, and the intensity of its DAS has been markedly reduced. Its peak wavelength has remained the same, as expected if a single class of residues is affected. Figure 4 shows the intensities associated with each DAS as a function of acrylamide concentration. The short-lived and intermediate-lived components remain constant in intensity over this range of quencher. The entire decrease in total S1 emission intensity is accounted for by the decrease in the long-lived component. At 0.05 M acrylamide the long lifetime has been reduced to 6.6 ns, and above this concentration it becomes too near the intermediate lifetime for the two to be accurately resolved. It is therefore not possible to calculate

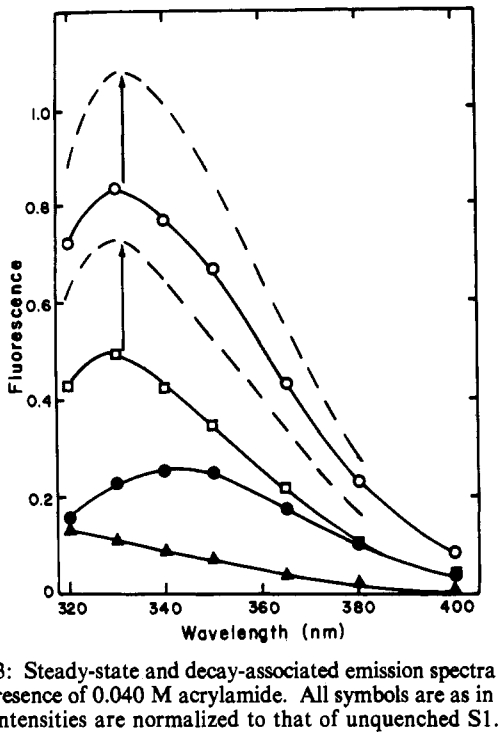

FIGURE 3: Steady-state and decay-associated emission spectra for S1 in the presence of 0.040 M acrylamide. All symbols are as in Figure 2, and intensities are normalized to that of unquenched S1.

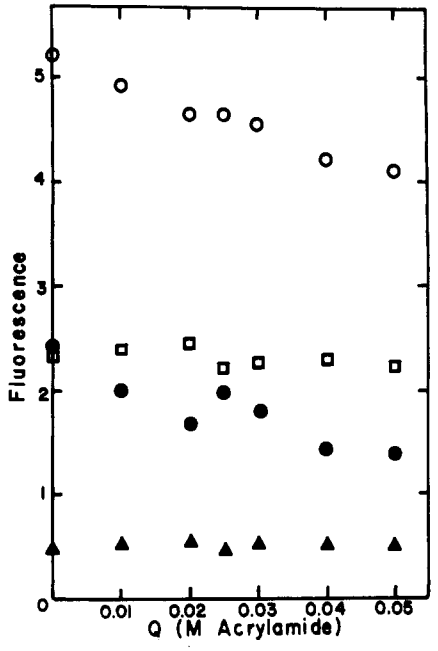

FIGURE 4: Intensities associated with the individual DAS as a function of acrylamide concentration. Symbols correspond to Figure 2.

the DAS above this concentration. Analysis of the two longer components according to the Stern–Volmer equation

$$I_0/I = 1 + K_{sv}[Q] \quad (5)$$

yields a quenching constant, K_{sv}, of 14.9 ± 2.9 M^{-1} for the long-lived component, while the intermediate lifetime component has a quenching constant not significantly different from zero. Analysis of the total intensity yields an apparent constant of 5.6 ± 0.5 M^{-1}, but this is invalid since the above results indicate a significant fraction of the intensity is unquenched. Although it is probably an oversimplification in this case, the assumption can be made that only two quenching classes exist, one totally inaccessible and one accessible, and then the analysis of Lehrer (1971) can be applied. The quenching of total S1 emission analyzed in this way is shown in Figure 5. The quenching constant is 12.6 ± 1.2 M^{-1}, the same within error as that obtained for the long component.

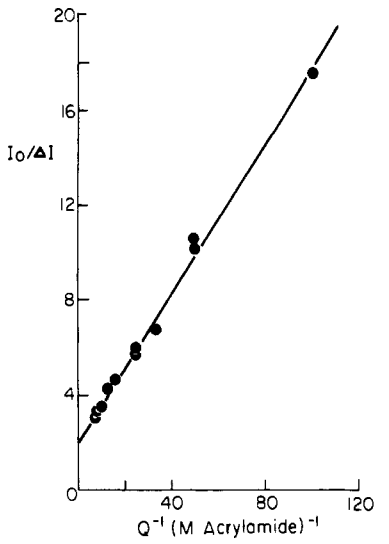

FIGURE 5: Modified Stern–Volmer plot of the quenching of the total intensity of S1 by acrylamide. Data are analyzed according to $I_0/\Delta I = 1/f_a + 1/(f_a K_{sv} Q)$, where f_a is the fraction of intensity accessible to the quencher (Lehrer, 1971).

Also, the relative contribution of the short, intermediate, and long components to the intensity in Figure 2 are 0.09, 0.45, and 0.46, respectively, while the fraction accessible to the quencher from Figure 5 is 0.504 ± 0.036, suggesting that the longest component accounts for essentially all of the quenchable class at low acrylamide concentrations. These results are in qualitative agreement with those reported by Onishi et al. (1973). Using iodide, they found about half the emission was quenchable. The quenchable class of residues had an emission maximum at approximately 350 nm and the nonquenchable class at 330 nm.

A second agent, magnesium–ATP, was also used to perturb the intrinsic emission of S1 tryptophans. Under the present conditions of buffer and temperature, the hydrolysis of ATP is slow, allowing the intensity to remain constant over the time interval required for data collection. After MgATP is added, the total emission intensity increases by about 17%. The DAS show that again the short component is unaffected. The intensity in the intermediate lifetime component has increased by 29%, however, and that of the long lifetime component by 9% (Figure 2). Within experimental error the three lifetimes, 0.74, 4.6, and 8.5 ns, are unchanged from those obtained in the absence of nucleotide. The ATP exerts its main influence on the intermediate component intensity, and the lack of effect on the lifetimes indicates that the mechanism is a ground-state, rather than an excited-state, process. The most plausible explanation is that the binding of ATP reduces the degree of static quenching of one or more "buried" tryptophans.

When the quenching of the intrinsic emission by acrylamide in the presence of ATP is examined, the reduction in intensity again occurs only in the long-lived component, while the enhancement in the intermediate lifetime component is unaffected (Figure 3). The dynamic quenching constant is now 25.2 ± 5.3 M^{-1}, apparently somewhat larger than that for S1 alone. However, testing for the homogeneity of the two slopes with Student's t test (Steel & Torrie, 1960) indicates that they are not significantly different ($P > 0.4$).

Discussion

The preceding analysis assumes that the derived decay-associated spectra are associated with individual tryptophans of S1. Since there are five tryptophans in the heavy chain, no one-to-one assignment is possible, but each tryptophan is

presumed to belong to one of three classes. Similar investigations on other proteins have demonstrated that even with such incomplete resolution useful information can be extracted. In the first place, the quantum yields of the individual tryptophans may vary widely. This is the case, for example, in lysozyme, where two of the six tryptophans contribute 70% of the emission. In S1 a similar simplification may exist. In the second place, it is often possible to associate an emission characteristic such as the DAS with individual tryptophans in the protein structure, based on auxiliary information, for instance, from chemical modification or X-ray crystal structural data. To date, most such experiments have been carried out on proteins with only one or two tryptophans and whose X-ray structure and sequence are both known. In liver alcohol dehydrogenase (Ross et al., 1981b; Knutson et al., 1982) this information combined with quenching, energy-transfer, and chemical modification studies has allowed identification of the two individual tryptophan residues with well-resolved lifetimes and decay-associated spectra. In S1, on the other hand, the only auxiliary information available currently is the primary sequence. No high resolution X-ray information is expected in the near future. This situation makes the association of individual tryptophan residues with spectral parameters both more nebulous and more useful. An example of the utility is the data presented here on the effect of ATP on the DAS. Steady-state intensity measurements are only capable of quantifying the fluorescence intensity increase, while the DAS reveal that this enhancement is composed of a relatively large increase in the intensity of mainly one class of emitters. Also, the binding of ATP affects an entirely different class of tryptophans from those quenchable by acrylamide, since in both the presence and absence of nucleotide only the long lifetime component is affected by the addition of the quencher. The middle component is unaffected over the range of acrylamide used here, regardless of nucleotide.

There are several possible analytical difficulties that influence the above analysis. One arises from the fact that even single fluorophores can give multiexponential decay behavior, due either to microheterogeneity in the protein structure or to excited-state reactions occurring on a time scale similar to the fluorescence decay. Examples of this situation are seen in the emission of substituted naphthols (Gafni et al., 1976; Laws & Brand, 1979) and in the single tryptophan residue of adrenocorticotropic hormone (Ross et al., 1981a). Given the complexity of the S1 structure, there is currently no way to evaluate the seriousness of this difficulty, although the lack of any negative preexponential terms, even at the red edge of the emission, reduces the likelihood of large contributions from excited-state reactions.

Another complication is the possible presence of static quenching. Eftink & Ghiron (1976) treat this by including a static quenching term in the Stern–Volmer equation

$$I_0/I = (1 + K_{sv}[Q])e^{V[Q]} \quad (6)$$

where V is the static quenching constant. Their data on several proteins indicate that a quenching rate constant, k_q, of between 1×10^9 and 4×10^9 M^{-1} s^{-1} is characteristic of exposed tryptophans. The data here yield k_q values (given by $K_{sv} = k_q\tau_0$) of 1.7 (±0.33) $\times 10^9$ for S1 alone and 2.96 (±0.63) $\times 10^9$ for S1 in the presence of MgATP, confirming the high degree of exposure of these residues. For this magnitude of k_q, Eftink and Ghiron find that plausible values of V are from 0 to 1. The quality of the data in the Stern–Volmer plots here does not justify a direct evaluation of V from eq 5. Choosing a value of 0.5 and reanalyzing the data of Figure 5 in this way, however, yield new K_{sv} values of 14.0 and 24.2 M^{-1} in the absence and presence of MgATP, respectively. The uncertainty in the degree of static quenching therefore adds a small uncertainty of the values of the Stern–Volmer constants but has no influence on the qualitative conclusions.

The above results can be compared with those of Yamada et al. (1981), who studied the exposure of the S1 tryptophan residues to the solvent using hydrogen–deuterium exchange. They divided the tryptophans into a fast-exchanging group and a slow-exchanging group. Both exchange much slower than free tryptophan in solution, and they concluded that all residues are at least partially buried and that all are rendered less accessible upon the addition of ATP. Comparison between hydrogen exchange and fluorescence is difficult, since the former method looks at all residues equally while the latter is weighted by the quantum yield of the individual residues. Apparently the change in the solvent accessibility of some of the tryptophans is not reflected in a change in their spectroscopic behavior, since the results presented show that only a fraction of the emission is altered by ATP.

Acknowledgments

I express my appreciation to Manuel F. Morales for his support and assistance in the performance of this work and to Ludwig Brand for sharing his nonlinear analysis software.

Registry No. Mg-ATP, 1476-84-2; tryptophan, 73-22-3; acrylamide, 79-06-1.

References

Ando, T., Duke, J. A., Tonomura, Y., & Morales, M. F. (1982) *Biochem. Biophys. Res. Commun. 109*, 1–6.

Badea, M. G., & Brand, L. (1979) *Methods Enzymol. 61*, 378–425.

Bagshaw, C. R., & Trentham, D. R. (1974) *Biochem. J. 141*, 331–349.

Beechem, J. M., Knutson, J. R., Ross, J. B. A., Turner, B. W., & Brand, L. (1983) *Biochemistry 22*, 6054–6058.

Bevington, P. R. (1969) *Data Reduction and Error Analysis for the Physical Sciences*, McGraw-Hill, New York, NY.

Chock, S. P., & Eisenberg, E. (1979) *J. Biol. Chem. 254*, 3229–3235.

Chock, S. P., Chock, P. B., & Eisenberg, E. (1979) *J. Biol. Chem. 254*, 3236–3243.

Donzel, B., Gauduchon, P., & Wahl, P. (1974) *J. Am. Chem. Soc. 96*, 801–808.

Dos Remedios, C. G., Yount, R. G., & Morales, M. F. (1972) *Proc. Natl. Acad. Sci. U.S.A. 69*, 2542–2546.

Eftink, M. R., & Ghiron, C. A. (1976) *Biochemistry 15*, 672–680.

Gafni, A., Modlin, R. L., & Brand, L. (1976) *J. Phys. Chem. 80*, 896–904.

Grinvald, A., & Steinberg, I. Z. (1974) *Anal. Biochem. 59*, 583–598.

Grinvald, A., & Steinberg, I. Z. (1976) *Biochim. Biophys. Acta 427*, 663–678.

Hozumi, T. (1981) *J. Biochem. (Tokyo) 90*, 785–788.

Inokuti, M., & Hirayama, F. (1965) *J. Chem. Phys. 43*, 1978–1989.

Johnson, K. A., & Taylor, E. W. (1978) *Biochemistry 17*, 3432–3442.

Kishi, K., & Noda, H. (1983) *J. Biochem. (Tokyo) 93*, 717–721.

Knutson, J. R., Walbridge, D. G., & Brand, L. (1982) *Biochemistry 21*, 4671–4679.

Knutson, J. R., Beechem, J. M., & Brand, L. (1983) *Chem. Phys. Lett. 102*, 501–507.

Laws, W. R., & Brand, L. (1979) *J. Phys. Chem. 83*, 795–802.

Lehrer, S. S. (1971) *Biochemistry 10*, 3254–3263.
Mendelson, R., Putnam, S., & Morales, M. (1975) *J. Supramol. Struct. 3*, 162–168.
Morita, F. (1967) *J. Biol. Chem. 242*, 4501–4506.
Onishi, H., Ohtsuka, E., Ikehara, M., & Tonomura, Y. (1973) *J. Biochem. (Tokyo) 74*, 435–450.
Privat, J.-P., Wahl, P., Auchet, J.-C., & Pain, R. H. (1980) *Biophys. Chem. 11*, 239–248.
Ross, J. B. A., Rousslang, K. W., & Brand, L. (1981a) *Biochemistry 20*, 4361–4369.
Ross, J. B. A., Schmidt, C. J., & Brand, L. (1981b) *Biochemistry 20*, 4369–4377.
Steel, R. G. D., & Torrie, J. H. (1960) *Principles and Procedures of Statistics*, McGraw-Hill, New York, NY.
Stein, L. A., Schwarz, R. P., Chock, P. B., & Eisenberg, E, (1979) *Biochemistry 18*, 3895–3909.
Tonomura, Y., Appel, P., & Morales, M. F. (1966) *Biochemistry 5*, 515–522.
Torikata, T., Forster, L. S., O'Neal, C. C., Jr., & Rupley, J. A. (1979) *Biochemistry 18*, 385–390.
Trybus, K. M., & Taylor, E. W. (1982) *Biochemistry 21*, 1284–1294.
Weeds, A. G., & Taylor, R. S. (1975) *Nature (London) 257*, 54–56.
Werber, M. M., Szent-Gyorgi, A. G., & Fasman, G. D. (1972) *Biochemistry 11*, 2872–2883.
Yamada, T., Shimizu, H., Nakanishi, M., & Tsuboi, M. (1981) *Biochemistry 20*, 1162–1168.

Structural Analysis of Myeloperoxidase by Resonance Raman Spectroscopy†

Scott S. Sibbett and James K. Hurst*

ABSTRACT: Soret excitation of canine myeloperoxidase (MPO) gives rise to a complex resonance Raman (RR) spectrum characterized by multiple bands in the core size and oxidation state marker regions. Relative intensities of the bands obtained by 406- and 454-nm laser excitation were nearly identical and were temperature independent from 77 to 273 K. Spectra of dithionite-reduced and cyanide-coordinated derivatives are also reported. In the native and dithionite-reduced enzyme, there are no detectable bands between 1620 and 1700 cm^{-1}, indicating that the hemes do not contain formyl substituents in conjugation with the macrocyclic ring. Excitation of the visible absorption band at 568 nm gave rise to only very weakly resonance-enhanced spectra. The RR spectra are interpreted within the context of other physical measurements to indicate that MPO contains two equivalent or nearly equivalent chlorin prosthetic groups. Possible mechanistic consequences of these structural features are discussed.

Myeloperoxidase (MPO)[1] has been implicated in the antimicrobial and cytotoxic reactions of neutrophils and monocytes (Klebanoff & Clark, 1978). This enzyme is functionally unique in its capacity to catalyze the peroxidation of chloride ion (Harrison & Schultz, 1976). The reaction produces hypochlorous acid (HOCl), whose ability to cause extremely rapid oxidative degradation of a wide variety of biological substrates, including porphyrins, hemes, and heme proteins (Albrich et al., 1981), suggests that it is the ultimate MPO-generated toxin (Klebanoff & Clark, 1978; Albrich et al., 1981).

The enzyme is dimeric (Andrews & Krinsky, 1981; Harrison et al., 1977; Olsson et al., 1972), containing two heme prosthetic groups (Agner, 1958) which bind small anions (Eglinton et al., 1982; Wever & Bakkenist, 1980; Harrison, 1979; Odajima & Yamazaki, 1972a) and react with hydrogen peroxide (Harrison et al., 1980). During turnover, MPO undergoes slow self-inactivation that is accompanied by chromophoric bleaching (Matheson et al., 1981), but this reaction is inhibited by addition of HOCl-reactive reagents (Naskalski, 1977). Apparently, therefore, the MPO active site is unusually constructed to provide self-protection during formation of the oxidant. The ability of the enzyme to generate large quantities of HOCl in the presence of oxidizable substrates and then inactivate when substrate is depleted may be critical to its proper functioning in the physiological environment. One can envision that phagosomal stimulation by invading pathogens leads to oxidative degradation primarily of internalized organisms, beyond which point HOCl production must be terminated to minimize damage to surrounding host tissues.

Attempts to identify the iron-containing chromophores have been frustrated by their chemical instability (Harrison & Schultz, 1978; Wu & Schultz, 1975; Nichol et al., 1969; Odajima & Yamazaki, 1972b; Newton et al., 1965a,b). The prosthetic groups are covalently linked to the protein (Wu & Schultz, 1975; Schultz et al., 1983). Under conditions examined thus far, cleavage has led to isolation of hemes with physical properties that are distinctly altered from the native enzyme (Harrison & Schultz, 1978; Wu & Schultz, 1975; Nichol et al., 1969). Structural identification has therefore relied principally upon inference from physical characteristics of the intact enzyme. Soret and visible absorption bands, especially of the reduced form, are dramatically red shifted compared to those of protoheme (Adar, 1978) and heme *c* containing peroxidases (Rönnberg et al., 1981). On the basis

† From the Department of Chemistry and Biochemical Sciences, Oregon Graduate Center, Beaverton, Oregon 97006. *Received December 29, 1983.* This work was supported by National Institutes of Health Grants AI 15834 and GM 31620.

[1] Abbreviations: MPO, myeloperoxidase (donor:H_2O_2 oxidoreductase, EC 1.11.1.7); RR, resonance Raman; EPR, electron paramagnetic resonance; MCD, magnetic circular dichroism.

0006-2960/84/0423-3007$01.50/0